Ultrasonic study of the magnetic phase diagrams of $CsNi_{0.98}M_{0.02}Cl_3$ (M = Co, Fe, Mg)

Y. Trudeau, M. L. Plumer, and M. Poirier
Centre de Recherche en Physique du Solide et Département de Physique, Université de Sherbrooke, Sherbrooke, Québec, Canada J1K 2R1

J. Takeuchi
Department of Physics, Shimane University, Matsue 690, Japan
(Received 31 January 1995; revised manuscript received 20 March 1995)

The phase diagrams of $CsNi_{0.98}M_{0.02}Cl_3$ (M = Mg, Co, and Fe) have been determined by ultrasonic velocity measurements. As expected, when comparing with pure $CsNiCl_3$, these systems show, respectively, enhanced Heisenberg, Ising, and XY effective single-ion anisotropy. The first two systems display phase diagrams with the same general features as $CsNiCl_3$, while with M = Fe, the system becomes an XY antiferromagnet like $CsMnBr_3$. A qualitative mean-field theory model for the paramagnetic phase boundary is also presented. This model has been used to understand the peculiar behavior of $CsNi_{0.98}Co_{0.02}Cl_3$ at high magnetic field.

I. INTRODUCTION

Over the last decade, extensive studies of the magnetic properties of the hexagonal insulators belonging to the ABX_3 family have been conducted.[1] In these systems, the magnetic ions B are grouped in $\hat{c}$-axis chains that are relatively isolated from each other by large A ions. This structural anisotropy causes the magnetic properties to have a strong quasi-one-dimensional (quasi-1D) behavior. The Hamiltonian describing such systems is

$$H = -2J_{\parallel}\sum_i \mathbf{S}_i\cdot\mathbf{S}_{i+1} - J_{\perp}\sum_{i\neq j}\mathbf{S}_i\cdot\mathbf{S}_j - D\sum_i (S_i^z)^2 - \mathbf{H}\cdot\sum_i \mathbf{S}_i\ , \quad (1)$$

where $J_{\parallel} < 0$ and $J_{\perp} < 0$ are the antiferromagnetic (AF) intra- and interchain nearest-neighbor exchange interactions, respectively. Parameter D is the single-ion anisotropy. If $D > 0$, the system has an easy-magnetization axis along $\hat{c}$, while if $D < 0$, the magnetization is energically favored if it stays in the basal plane, perpendicular to $\hat{c}$. A quasi-1D system is defined by $|J_{\parallel}/J_{\perp}| \gg 1$.

In many ABX_3 systems, D and $J_{\perp}$ have approximately the same magnitude and competition arises between these two interactions. The triangular arrangement of the hexagonal lattice of these compounds also adds to the complexity of the problem by introducing frustration in the case of AF coupling, $J_{\perp} < 0$. In addition, D and $J_{\perp}$ are usually not too large and reasonable magnetic fields can alter the balance between these competing interactions and induce transitions.

Several ABX_3 systems with weak axial anisotropy exhibit similar phase diagrams.[2] An example is $CsNiCl_3$.[3–5] with parameters of the Hamiltonian (1), as reported by Buyers *et al.*,[6] given by $J_{\parallel}/k_B = -16.6$ K, $J_{\perp}/k_B = -0.29$ K, and $D/k_B = 0.63$ K. At low temperatures, the competition between these interactions and a magnetic field oriented along the $\hat{c}$ axis gives rise to four magnetic phases which share a common tetracritical point located at $T_{mc} = 4.48$ K and $\mathbf{H}_{mc} = 2.1$ T. Many other systems, like $CsNiBr_3$ and $CsMnI_3$,[3] have similar phase diagrams and it can be shown that they superimpose relatively well when the critical fields and temperatures are normalized;[3] differences arise only from the relative sizes of D, $J_{\perp}$.

In $CsNiCl_3$, Takeuchi *et al.*[7] have shown that it is possible to effectively alter the value of the single-ion anisotropy D by substituting a certain amount of Ni^{2+} by ions with different anisotropy. These local changes in single-ion anisotropy are then spread through the chains by the large intrachain interaction $J_{\parallel}$. In zero field, their specific heat measurements have shown that critical-temperature modifications can be explained by a global variation of D. Since the overall value of D is modified, changes in the rest of the phase diagram are also expected. As an example, in an easy-axis system like $CsNiCl_3$, the spin-flop field H_{SF} is directly related to D.[8] So this left an open question: Will the whole phase diagram be consistent with this simple scheme?

The present study addresses this problem and we present an experimental determination, by acoustic velocity, of the magnetic phase diagrams of $CsNi_{0.98}Mg_{0.02}Cl_3$, $CsNi_{0.98}Co_{0.02}Cl_3$, and $CsNi_{0.98}Fe_{0.02}Cl_3$. According to the previous results of Takeuchi *et al.*,[7] it is expected that these susbstitutions will produce systems with enhanced Heisenberg, Ising, and XY behavior, respectively. These results will then be compared with the phase diagram of the pure system and, when possible, to other relevant ABX_3 systems. Some particularities of the high-field part of the $CsNi_{0.98}Co_{0.02}Cl_3$ phase diagram have also led us to include results of a qualitative mean-field theory model

based on the 1D transfer matrix method.

It is our experience[4,9,5] that ultrasound is a very effective and economical way of studying the magnetic properties of such systems. The basics of this experimental technique have already been presented by Trudeau *et al.* in Ref. 5, and so no further description will be given here. Before presenting, in Sec. II, the phase diagrams of the mixed compounds as obtained by ultrasound, a brief review of the phase diagram of the pure system is given in order to provide a basis for comparison. Finally, results of a qualitative mean-field tranfer-matrix model at high field are presented in Sec. IV.

II. RESULTS AND DISCUSSION

The procedure used to set critical fields and temperatures from the anomalies on $\Delta v/v$ is similar to the one found in Ref. 5 for pure $CsNiCl_3$. Following this procedure, critical points are defined where the variation of the acoustic velocity is the largest. This corresponds to the large changes experienced by the magnetic part of the system at a phase transition. The correctness of this choice is confirmed by the good agreement of the critical points for both the temperature and magnetic field sweeps. Some examples of acoustic velocity as a function of temperature in zero field and the related choice of transition points are presented in Fig. 1 for $CsNi_{0.98}Mg_{0.02}Cl_3$ and $CsNi_{0.98}Co_{0.02}Cl_3$.

Before discussing the mixed compounds, it is instructive to review the magnetic phase diagrams of pure $CsNiCl_3$.[5] These are presented in Figs. 2 and 3, for $\mathbf{H} \parallel \hat{c}$ and $\mathbf{H} \perp \hat{c}$, respectively. In zero field, two magnetic phases can be observed. As the temperature is lowered from the paramagnetic phase P, the easy-axis anisotropy aligns the spins along the hexagonal $\hat{c}$ axis at $T_{N1} \simeq 4.8$ K. This gives a linear antiferromagnetic phase L that partly frustrates $J_\perp$. A further reduction of temperature will eventually cause a sharing of this frustration between $J_\perp$ and D. This happens at $T_{N2} \simeq 4.4$ K where additional basal-plane ordering occurs, causing an elliptical 120° phase E. In the E phase, the spins lie in a plane which includes the hexagonal axis. The application of a field along this axis adds another frustation to the system. This time, the frustration is between the field and D. At high enough field, it is more favorable for spins to frustrate D and they adopt a helical 120° structure in a plane which is now perpendicular to the hexagonal axis (and $\mathbf{H}$). This phase is the spin-flop phase SF. These magnetic phases are found to coexist at a multicritical point which is located for this system at $H_{\rm mc} \simeq 2.1$ T and $T_{\rm mc} \simeq 4.48$ K. The situation is much different when the field is perpendicular to the chain axis since there is no longer competition between the easy-axis anisotropy D and the magnetic field. This causes, as it can be observed in Fig. 3, the disappearence of the spin-flop phase and of the multicritical point.

Since the percentage of substituted magnetic ions is rather small (2%), only small modifications to the phase diagram are expected. This is exactly what has been observed for two of the three mixed compounds,

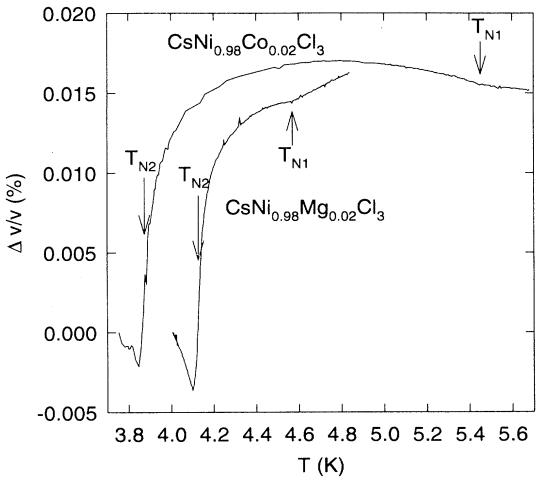

FIG. 1. Acoustic velocity data as a function of temperature in zero magnetic field for $CsNi_{0.98}Co_{0.02}Cl_3$ and $CsNi_{0.98}Mg_{0.02}Cl_3$. The arrows indicate where the transition points are chosen.

$CsNi_{0.98}Mg_{0.02}Cl_3$ and $CsNi_{0.98}Co_{0.02}Cl_3$. These phase diagrams are presented in Figs. 2 and 3 for $\mathbf{H} \parallel \hat{c}$ and $\mathbf{H} \perp \hat{c}$, respectively.

As mentioned above, the principal effect of the substitution of ions at the Ni sites is to modify the value of the effective single-ion anisotropy D. In the case of a substitution with Mg ions, since $CsMgCl_3$ is nonmagnetic, it is reasonable to expect a dilution of D and a more Heisenberg-like system. As a result, since the magnitude of $H_{\rm SF}$ is linked to D,[8] a smaller spin-flop field is expected. The single-ion anisotropy is also responsible for the onset of the linear phase,[2] and so the T_{N1} should be smaller. These predictions are confirmed by the magnetic phase diagrams of $CsNi_{0.98}Mg_{0.02}Cl_3$ shown in Figs. 2 and 3. For this compound, the two observable magnetic

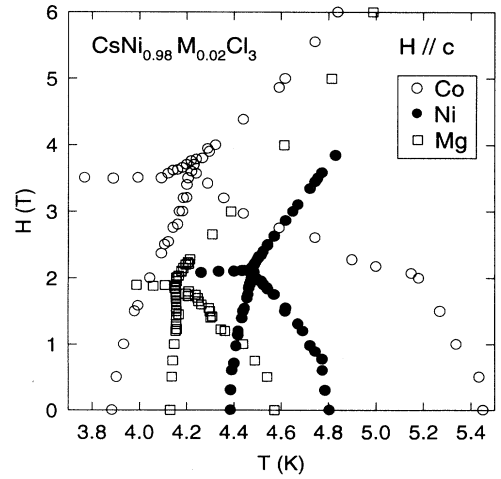

FIG. 2. Magnetic phase diagrams of $CsM_{0.02}Ni_{0.98}Cl_3$ as determined from acoustic velocity anomalies for $\mathbf{H} \parallel \hat{c}$. The open circles, squares, and the solid circles represent M = Co, Mg, and Ni (Ref. 5), respectively.

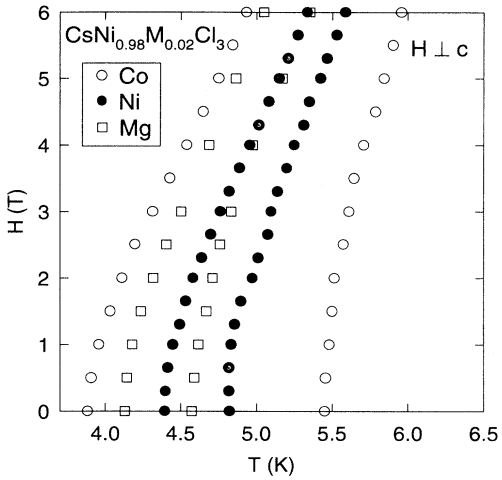

FIG. 3. Magnetic phase diagrams of $CsM_{0.02}Ni_{0.98}Cl_3$ as determined from acoustic velocity anomalies for $\mathbf{H} \perp \hat{c}$, labeled as in Fig. 2.

phase transitions in zero field are at $T_{N1} \simeq 4.57$ K and $T_{N2} \simeq 4.13$ K and the multicritical point for $\mathbf{H} \parallel \hat{c}$ is located at $T_{\rm mc} \simeq 4.16$ K and $H_{\rm mc} \simeq 1.9$ T. The zero-field critical temperatures are in agreement with the results reported by Takeuchi *et al.*[7] The overall shape of these diagrams are the same as the ones of pure system but the spin-flop field is approximately 10% smaller and T_{N1} more than 0.2 K lower. One can also observe the relative displacement, as a function of temperature, of the multicritical point with respect to T_{N2}. In the pure system, $T_{\rm mc} - T_{N2} \simeq 0.1$ K, while with Mg doping, this difference is reduced to 0.02 K. This is reasonable, since a system with a smaller D has more freedom and it requires a lower temperature to induce order. As a result, the whole transition line is displaced toward lower temperatures. The behavior of T_{N2} is much less obvious. If the easy-axis single-ion anisotropy was simply turned off in $CsNiCl_3$, it should present only one critical temperature somewhere between the original two. This is not happening in $CsNi_{0.98}Mg_{0.02}Cl_3$, where T_{N2} is lower than in $CsNiCl_3$. This behavior can only be explained by a slight reduction of the effective $J_\perp$ caused by the substitution of nonmagnetic Mg atoms.

In the $CsNi_{0.98}Co_{0.02}Cl_3$ compound, the behavior is the opposite from $CsNi_{0.98}Mg_{0.02}Cl_3$. This is due the Ising single-ion anisotropy of the Co ions as is well known from the strong Ising behavior of $CsCoCl_3$.[10] Following the same argument as the one used for $CsNi_{0.98}Mg_{0.02}Cl_3$, one can predict a higher spin-flop field and T_{N1}. Since an enhanced Ising single-ion anisotropy favors phase L, we can also expect a lower T_{N2}. This is observed in Figs. 2 and 3. For this system, the zero-field transition temperatures are $T_{N1} \simeq 5.46$ K and $T_{N2} \simeq 3.88$ K. Compared to the undoped compound, it represents an increase for T_{N1} of more than 0.8 K and a decrease of T_{N2} of more than 0.5 K. The situation is similar with $H_{\rm SF}$; instead of 2.1 T for $CsNiCl_3$, it now rises up to 3.5 T. All these phenomena are consistent with an increase of the effective easy-axis single-ion anisotropy.

This increase of single-ion anisotropy, caused by the substitution of Co ions at the Ni sites, also has an effect on the shapes of the E-L and SF-P phase boundaries. In the first case, this is manifest by the large difference between $T_{\rm mc}$ and T_{N2}, $T_{\rm mc}$ being more than 0.3 K greater than T_{N2}. Reversing the argument used for $CsNi_{0.98}Mg_{0.02}Cl_3$, one can conclude that the enhanced Ising anisotropy helps to order the system by reducing its degrees of freedom, and so the L phase can stabilize at a higher temperature. For the SF-P line, the field and the easy-axis single-ion anisotropy tend to destroy the spin-flop phase by their tendency to align the spins along the chain axis. Evidence of this is found in Fig. 4 where the phase diagram of $CsNi_{0.98}Co_{0.02}Cl_3$ for $\mathbf{H} \parallel \hat{c}$ is presented for fields up to 14 T. With the help of the straight line, it is easy to observe the curvature of the SF-P phase boundary, favoring the paramagnetic phase to the detriment of the spin-flop phase at high field. From this curvature, it can be expected that for a field larger than 25–30 T, the critical temperature T_C will decrease as a function of field. At such high magnetic field ($H/g\mu_B \sim J_\parallel$), the transverse susceptibilty, reponsible for the magnetic order,[19] is reduced by the tilting of the spins toward the field. Eventually, for a large enough magnetic field, there will be no more SF phase.[15] The same experiment has been conducted for $CsNiCl_3$ and a similar curvature, altough far less pronounced, has also been observed. Further dicussions of this behavior will be presented in the next section where an outline of the high-field transfer-matrix results will be given.

The last compound investigated is $CsNi_{0.98}Fe_{0.02}Cl_3$. Inside an ABX_3 matrix, the Fe ions are known to exhibit a strong XY behavior, as in $RbFeCl_3$.[11] In fact, since the Ising-like behavior of $CsNiCl_3$ is weak, a total suppression of this type of anisotropy is possible. So, instead of phase diagrams having the general features of $CsNiCl_3$, they will present the characteristics of an AF chains sys-

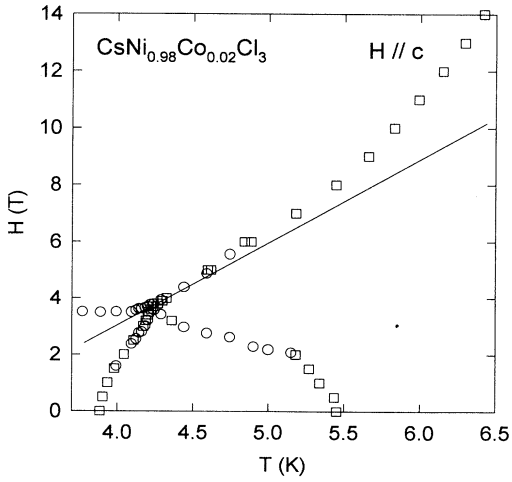

FIG. 4. High-field part of the magnetic phase diagrams of $CsCo_{0.02}Ni_{0.98}Cl_3$ as determined from acoustic velocity anomalies for $\mathbf{H} \parallel \hat{c}$. The straight line emphasizes the upward curvature of the high-field transition line.

tem with XY anisotropy and AF coupling on a triangular lattice such as $CsMnBr_3$ (Refs. 12, 13) and $RbMnBr_3$.[14] This behavior can be observed in Figs. 5 and 6 where the magnetic phase diagrams of $CsNi_{0.98}Fe_{0.02}Cl_3$ for $\mathbf{H} \parallel \hat{c}$ and $\mathbf{H} \perp \hat{c}$ are presented. As with other XY systems,[13,14] $CsNi_{0.98}Fe_{0.02}Cl_3$ shows only two magnetic phases for $\mathbf{H} \parallel \hat{c}$ with $T_N \simeq 4.58$ K. At low temperature, the XY confinement caused by the Fe ions generates a planar 120° order whose symmetry is similar to the spin-flop phase of $CsNiCl_3$. As a function of field, this spin confinement in the XY plane is enhanced by the AF coupling along the chains, causing an increase of the critical temperature. For $\mathbf{H} \perp \hat{c}$, the picture is somewhat different, as shown in Fig. 6. The phase diagram is now made of at least three magnetic phases. In order to avoid confusion in the labeling of these phases, the notation of Plumer *et al.*[2] will be used. At low field and temperature there is a distorted XY planar 120° phase, labeled as 7, while at higher field, a phase transition occurs. Depending on the magnitude of $D/J_\perp$ this phase is labeled either 3 or 5.[15] Of course, at high temperature the magnetic phase for both field orientations is paramagnetic (phase 1).

If the value of D is large compared to $J_\perp$, like in $CsMnBr_3$,[16] the spins are confined to the basal plane and one of the three magnetic sublattices will turn along one of the other two directions at the phase transition. This corresponds to the description of phase 5 of Plumer *et al.*[2] and it implies the frustration of $J_\perp$. On the contrary, if the ratio is small,[14] like in $RbMnBr_3$, the spins will flop outside of the basal plane and D will be frustrated. This phase is labeled as 3 and is similar to the elliptical phase of $CsNiCl_3$. From its origin, it is reasonable to expect a small $D/J_\perp$ ratio for $CsNi_{0.98}Fe_{0.02}Cl_3$, but this would imply the presence of the fourth magnetic phase[14,2] 3. However, no evidence of a 3-5 phase boundary has been found in $CsNi_{0.98}Fe_{0.02}Cl_3$, although a discontinuity is present at the boundary of phase 7, which could indicate the presence of a multicritical point. The arrow in Fig. 6 indicates this discountinuity.

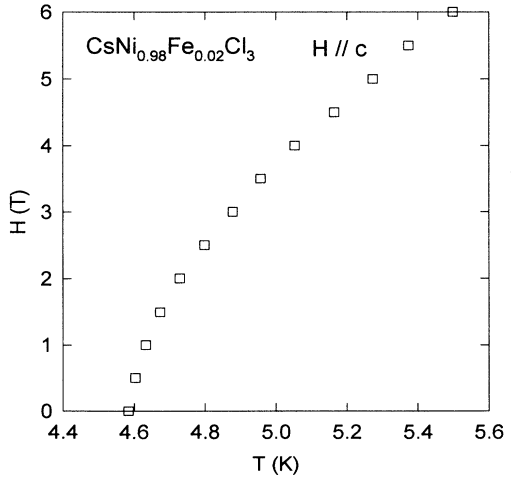

FIG. 5. Magnetic phase diagram of $CsNi_{0.98}Fe_{0.02}Cl_3$ as determined from acoustic velocity anomalies for $\mathbf{H} \parallel \hat{c}$ obtained from constant field sweeps.

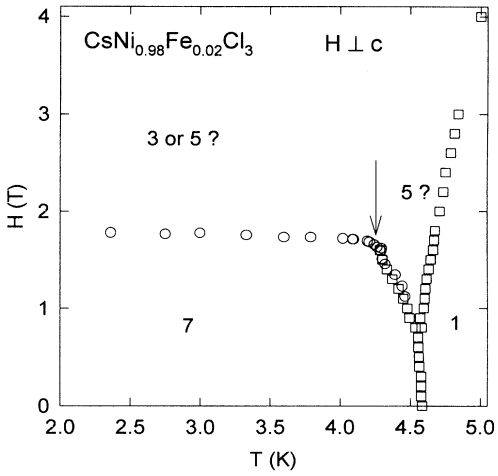

FIG. 6. Magnetic phase diagram of $CsNi_{0.98}Fe_{0.02}Cl_3$ as determined from acoustic velocity anomalies for $\mathbf{H} \perp \hat{c}$. The squares are critical temperatures obtained at constant field and the circles are critical fields obtained at constant temperature. Phases are labeled as in Ref. 2.

At lower Fe concentration, it is reasonable to expect the recovery of the easy-axis behavior. Takeuchi *et al.*[17] have recently found the critical concentration to be close to 0.7%.

III. HIGH-FIELD TRANSFER-MATRIX RESULTS

An attempt is made here to explain the rather unusual behavior observed in the high-field transition line of $CsNi_{0.98}Co_{0.02}Cl_3$. Although it is difficult to predict theoretically the entire diagram of such systems, it is simple to obtain at least a qualitative description of the transition lines to the paramagnetic phase (P). This simplification comes from the fact that linear response theory in the P phase can be used. In addition, the quasi-1D nature of these systems invites the use of 1D transfer-matrix techniques with 3D mean-field coupling.[18]

For a quasi-1D antiferromagnetic system, one can write a general expression for the 3D susceptibility at $\mathbf{q} = \pi$ as[19]

$$\chi_{3D}(\pi) = \frac{\chi_{1D}(\pi)}{1 - \alpha J_\perp \chi_{1D}(\pi)}, \tag{2}$$

where α is a constant dependent on the underlying magnetic and crystalline structure of the system. In systems like $CsNiCl_3$, the competition between $J_\perp$ and D makes the evaluation of this constant nontrivial.

The staggered susceptibility $\chi_{3D}(\pi)$ diverges at the paramagnetic phase boundary. In general, one must consider the components of the susceptibility $\chi^{\alpha\beta}$, where $\alpha, \beta = x, y, z$. As an example, at the border between the linear AF phase L and the paramagnetic phase P, $\chi^{zz}(\pi)$

will diverge since the ordering in phase L is along the z axis (the hexagonal $\hat{\mathbf{c}}$ axis). Similarily, at the transition line separating the SF phase from the P phase, the spins are in the plane perpendicular to z, and so the $\chi^{xx}(\pi)$ [or $\chi^{yy}(\pi)$] component can be considered.

Since the ordering mechanisms in phases L and SF are different, there is no reason why the constant α of Eq. (2) should be the same for both. As the goal of the present model is only to give a qualitative description of the lines bordering the paramagnetic phase, this constant will be set arbitrarily.

Results of transfer-matrix calculations for χ_{1D} as a function of a magnetic field[20–23,5] along the z axis are presented in Fig. 7 for an $S = 1$ system with $J_{\|} = -1$ and $D/|J_{\|}| = 0.02$. From top to bottom, these susceptibility plots were obtained for, respectively, $T/|2J_{\|}| = 0.03$, 0.035, 0.04, 0.045, and 0.05. At low field, the easy magnetization axis caused by the anisotropy term is clearly evident from the high value of the z component of the susceptibility, χ^{zz}. As the field is increased, this component falls rather rapidily, especially when the spins flop to the plane at $H \sim 0.5$. This spin-flop field value, although controlled by D, is extremely large in transfer-matrix calculations. This comes from the fact that in systems like $CsNiCl_3$ the competition between $J_{\perp}$ and D tends to reduce the effective anisotropy. Since only a qualitative description is attempted here, this discrepancy is not relevant. Of course, as the spins flop to the plane, the transverse component χ^{xx} increases drastically. Further increase in the field helps confine the spins to the plane and χ^{xx} continues to rise up to a point where $J_{\|}$ is no longer able to compete against the field. At such high field, the spins start to tilt toward the field direction and their projections in the plane is reduced along with χ^{xx}.

With all these elements in mind, one can start to look at the behavior of the transition lines bordering the paramagnetic phase, i.e., at the divergence of χ_{3D}. A straight horizontal line has been plotted in the upper part of Fig. 7. Since there is no easy way of calculating the constant α in Eq. (2), it will be supposed, in order to give a qualitative argument, that this line corresponds to the appropriate values of $\ln(1/\alpha J_{\perp})$ for both transitions lines. According to peculiar scales used for χ^{xx} and χ^{zz}, this implies that these constants are not the same.

Let us first consider the behavior of the L-P line. For this transition, the critical points are given by the intersection of the χ^{zz} plots (dotted lines) with the straight line. As expected, at low temperature the critical-field value is close to the spin-flop field, but as the temperature increases, it moves toward zero. Things becomes more interesting when one looks for the other phase boundary, separating the SF and P phases, as determined by the χ^{xx} plots. One can observe that these curves always intersect the horizontal line twice, once at low field corresponding to the usual transition, labeled as H_C in the literature,[5,2] and again at very high field, when the susceptibility is too much reduced to keep the system ordered. Just to give an approximate order of magnitude for this second critical field, in $CsNiCl_3$ where $J_{\|} = 16.6$ K,[6] this gives for $H \sim 6|J_{\|}|$ a field value in the neighborhood of 150 T. This estimate compares well with the $T = 0$ field value of 200 T from the work of Chubukov[15] when it is kept in mind that at $T = 0$, the susceptibility must be zero to prevent the ordering. This occurs when there is no spin projection in the plane.

Finally, consider the larger curvature observed on the high-field SF-P line of $CsNi_{0.98}Co_{0.02}Cl_3$. An element of this behavior is found in Fig. 8 where the transverse susceptibility $X^{xx}(\pi)$ is plotted as a function of field for various values of single-ion anisotropy D at $T = 0.03\ |2J_{\|}|$. In terms of D, the largest anisotropy $D = 0.1|J_{\|}|$ gives the highest spin-flop field and the largest zero-field χ^{zz}. Although it not very obvious at this temperature, the maximum of χ^{xx} for $D = 0.1\ |J_{\|}|$ is slightly lower than for the other anisotropies. This, coupled with rounding effect of temperature (see Fig. 7), causes a larger curvature of the SF-P boundary for systems with enhanced Ising anisotropy. Another phenomenon can also be observed. At high field the Ising anisotropy helps the field in frustrating $J_{\|}$ so that the transverse component of the sus-

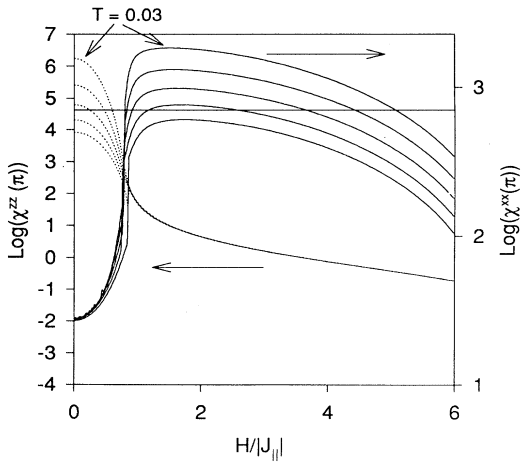

FIG. 7. Magnetic susceptibility χ_{1D} as a function of field for $D = 0.02|J_{\|}|$ and $T = 0.03|2J_{\|}|$, $0.035|2J_{\|}|$, $0.04|2J_{\|}|$, $0.045|2J_{\|}|$, and $0.05|2J_{\|}|$. The dotted and solids curves represent $\chi^{zz}(\pi)$ and $\chi^{xx}(\pi)$, respectively.

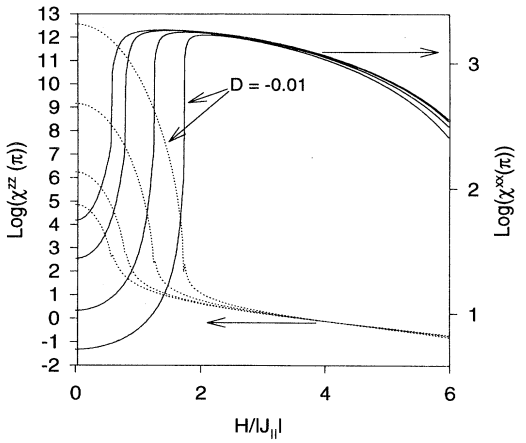

FIG. 8. Magnetic susceptibility χ_{1D} for $T = 0.03|2J_{\|}|$ and $D = 0.01|J_{\|}|$, $0.02|J_{\|}|$, $0.05|J_{\|}|$, and $0.1|J_{\|}|$. The dotted and solids curves represent $\chi^{zz}(\pi)$ and $\chi^{xx}(\pi)$, respectively.

ceptibitliy decreases more rapidily when the anisotropy is large. One can speculate that this will lower the second critical field for a given temperature.

IV. CONCLUSIONS

The phase diagrams of mixed compounds $CsNi_{0.98}Mg_{0.02}Cl_3$, $CsNi_{0.98}Co_{0.02}Cl_3$, and $CsNi_{0.98}Fe_{0.02}Cl_3$ for $\mathbf{H} \parallel \hat{c}$ and $\mathbf{H} \perp \hat{c}$ have been determined from acoustic velocity anomalies. The phase diagrams of the first two systems have been found to be very similar to that of pure $CsNiCl_3$ when accounting for enhanced Heisenberg and Ising effective single-ion anisotropies, respectively. The main effects of the variations of single-ion anisotropy have been observed in T_{N1} and H_{SF}. When compared to pure $CsNiCl_3$, these quantities have been found to be lower for $CsNi_{0.98}Mg_{0.02}Cl_3$ and higher for $CsNi_{0.98}Co_{0.02}Cl_3$. Another important feature of the phase diagram of $CsNi_{0.98}Co_{0.02}Cl_3$ for $\mathbf{H} \parallel \hat{c}$ is the curvature of the phase boundary between the spin-flop and the paramagnetic phases at high field. This enhanced curvature is due to the stronger Ising single-ion anisotropy of $CsNi_{0.98}Co_{0.02}Cl_3$. From this curvature, it can be expected that for fields higher than 25–30 T, the critical temperature will decrease as a function of field. A mean-field model which uses one-dimensional susceptibility results of a classical transfer matrix has also been presented. Qualitatively, this model reproduces all the observed features of the paramagnetic phase boundaries.

The phase diagrams of $CsNi_{0.98}Fe_{0.02}Cl_3$ are different from those of $CsNiCl_3$. In this compound, the strong XY character of the Fe ions completely changes the nature of the magnetic anisotropy. Instead, the comparison has been made with AF XY systems like $CsMnBr_3$ and $RbMnBr_3$, and once again the general features of these phase diagrams have been found to be very similar. At lower Fe concentration, however, the easy-axis anisotropy should be recovered.

This study clearly shows the effectiveness of the use of mixed $AB_{1-x}M_xX_3$ magnetic systems in the study of magnetic phase diagrams. It has been clearly established that a small subsitution of magnetic ions can modify the amplitude, or even the sign, of the effective single-ion anisotropy and provides a powerful basis for testing theoretical models dependent on single-ion anisotropy in a large class of magnetic systems.

ACKNOWLEDGMENTS

Financial support from the Centre de Recherche en Physique du Solide, the Natural Sciences and Engineering Research Council of Canada, and le Fonds pour la Formation de Chercheurs et l'Aide à la Recherche du Gouvernement du Québec has been essential for this work. We also thank M. Castonguay for technical assistance.

[1] *Magnetic Systems with Competing Interactions*, edited by H. T. Diep (World Scientific, Singapore, 1994).
[2] M. L. Plumer, K. Hood, and A. Caillé, Phys. Rev. Lett. **60**, 45 (1988); M. L. Plumer, A. Caillé, and K. Hood, Phys. Rev. B **39**, 4489 (1989).
[3] H. A. Katori, T. Goto, and Y. Ajiro, J. Phys. Soc. Jpn. **62**, 743 (1993).
[4] M. Poirier, A. Caillé, and M. L. Plumer, Phys. Rev. B **41**, 4869 (1990).
[5] Y. Trudeau, M. L. Plumer, M. Poirier, and A. Caillé, Phys. Rev. B **41**, 12 805 (1993).
[6] W. J. L. Buyers, R. M. Morra, R. L. Armstrong, M. J. Hogan, P. Gerlach, and K. Hirakawa, Phys. Rev. Lett. **56**, 371 (1986); R. M. Morra, W. J. Buyers, R. L. Armstrong, and K. Hirakawa, Phys. Rev. B **38**, 543 (1988).
[7] J. Takeuchi, T. Wada, I. Hiromitsu, and T. Ito, Solid State Commun. **87**, 899 (1993).
[8] R. M. White, *Quantum Theory of Magnetism*, 2nd ed. (Springer-Verlag, New York, 1983), p. 114.
[9] Y. Trudeau, M. Poirier, and A. Caillé, Phys. Rev. B **46**, 169 (1992).
[10] M. Meketa and K. Adachi, J. Phys. Soc. Jpn. **44**, 806 (1978).
[11] H. Yoshisawa, W. Kozukue, and H. Hirakawa, J. Phys. Soc. Jpn. **49**, 144 (1980).
[12] B. D. Gaulin, T. E. Mason, M. F. Collins, and J. A. Larese, Phys. Rev. Lett. **62**, 1380 (1989).
[13] A. Caillé, M. L. Plumer, M. Poirier, and B. D. Gaulin, Physica B **165 & 166**, 169 (1990); M. Poirier, M. Castonguay, A. Caillé, M. L. Plumer, and B. D. Gaulin, *ibid.* **165 & 166**, 171 (1990).
[14] L. Heller, M. F. Collins, Y. S. Yang, and B. Collier, Phys. Rev. B **49**, 1104 (1994).
[15] A. V. Chubukov, J. Phys. C **21**, L441 (1988).
[16] B. D. Gaulin, M. F. Collins, and W. J. L. Buyers, J. Appl. Phys. **61**, 3409 (1987).
[17] J. Takeuchi *et al.* (unpublished).
[18] Y. Trudeau and M. L. Plumer, Phys. Rev. B **51**, 5868 (1995).
[19] D. J. Scalapino, Y. Imry, and P. Pincus, Phys. Rev. B **11**, 2042 (1975).
[20] M. Blume, P. Heller, and N. A. Lurie, Phys. Rev. B **11**, 4483 (1975).
[21] J. M. Loveluck, J. Phys. C **12**, 4251 (1979).
[22] J.-G. Demers and A. Caillé, Solid State Commun. **68**, 859 (1988).
[23] Y. Trudeau, A. Caillé, M. Poirier, and J.-G. Demers, Solid State Commun. **82**, 825 (1992).